ADVANCES IN ATMOSPHERIC SCIENCES, VOL. 35, JUNE 2018, 737–752

• **Original Paper** •

Subseasonal Reversal of East Asian Surface Temperature Variability in Winter 2014/15

Xinping XU*[1], Fei LI[1,2,3], Shengping HE[1,2,4,5], and Huijun WANG[1,2,4]

[1]*Collaborative Innovation Center on Forecast and Evaluation of Meteorological Disasters/Key Laboratory of Meteorological Disaster, Ministry of Education, Nanjing University of Information Science and Technology, Nanjing* 210044*, China*

[2]*Nansen-Zhu International Research Center, Institute of Atmospheric Physics, Chinese Academy of Sciences, Beijing* 100029*, China*

[3]*NILU-Norwegian Institute for Air Research, Kjeller* 2007*, Norway*

[4]*Climate Change Research Center, Chinese Academy of Sciences, Beijing* 100029*, China*

[5]*Geophysical Institute, University of Bergen and Bjerknes Centre for Climate Research, Bergen* 5007*, Norway*

(Received 18 March 2017; revised 24 October 2017; accepted 21 November 2017)

ABSTRACT

Although there has been a considerable amount of research conducted on the East Asian winter-mean climate, subseasonal surface air temperature (SAT) variability reversals in the early and late winter remain poorly understood. In this study, we focused on the recent winter of 2014/15, in which warmer anomalies dominated in January and February but colder conditions prevailed in December. Moreover, Arctic sea-ice cover (ASIC) in September–October 2014 was lower than normal, and warmer sea surface temperature (SST) anomalies occurred in the Niño4 region in winter, together with a positive Pacific Decadal Oscillation (PDO|+) phase. Using observational data and CMIP5 historical simulations, we investigated the PDO|+ phase modulation upon the winter warm Niño4 phase (autumn ASIC reduction) influence on the subseasonal SAT variability of East Asian winter. The results show that, under a PDO|+ phase modulation, warm Niño4 SST anomalies are associated with a subseasonal delay of tropical surface heating and subsequent Hadley cell and Ferrel cell intensification in January–February, linking the tropical and midlatitude regions. Consistently, the East Asian jet stream (EAJS) is significantly decelerated in January–February and hence promotes the warm anomalies over East Asia. Under the PDO|+ phase, the decrease in ASIC is related to cold SST anomalies in the western North Pacific, which increase the meridional temperature gradient and generate an accelerated and westward-shifted EAJS in December. The westward extension of the EAJS is responsible for the eastward-propagating Rossby waves triggered by declining ASIC and thereby favors the connection between ASIC and cold conditions over East Asia.

Key words: East Asia, subseasonal temperature, Arctic sea-ice, Niño4 SST, Pacific Decadal Oscillation

Citation: Xu, X. P., F. Li, S. P. He, and H. J. Wang, 2018: Subseasonal reversal of East Asian surface temperature variability in winter 2014/15. *Adv. Atmos. Sci.*, **35**(6), 737–752, https://doi.org/10.1007/s00376-017-7059-5.

1. Introduction

The East Asian winter climate can be significantly influenced by the monsoon system, which includes the Siberian high (SH), the Aleutian low, the East Asian trough, and the East Asian jet stream (EAJS) (Chen and Sun, 1999; Wang and Jiang, 2004; Li and Yang, 2010). The expansion of the SH is associated with more intense northerly winds along coastal East Asia, leading to cold surges in the East Asian winter (Wu and Wang, 2002; He and Wang, 2012). An accelerated EAJS is usually accompanied by a deepened East Asian trough and Aleutian low, resulting in stronger low-level northerlies and hence cold-air advection to East Asia (Yang et al., 2002; Jhun and Lee, 2004).

Previous studies have shown that sea surface temperature (SST) variability in the tropical Pacific (Wang et al., 2000; He et al., 2013; Jin et al., 2016), North Pacific (He and Wang, 2013b; Ye and Chen, 2016), and Indian Ocean (Yang et al., 2010) is closely associated with the East Asian winter monsoon (EAWM) system. Wang et al. (2000) once revealed that El Niño events cause a weaker than normal EAWM and predominantly warm conditions over East Asia through a Pacific–East Asian teleconnection pattern. However, recent studies have demonstrated that the interannual relationship between the El Niño–Southern Oscillation (ENSO) and EAWM clearly undergoes a low-frequency oscillation and weakened around the mid-1970s (Wang and He, 2012; He and Wang, 2013a; He et al., 2013). Furthermore, it has been noted that the Pacific Decadal Oscillation (PDO) ex-

* Corresponding author: Xinping XU
Email: xuxinping1995@163.com

erts an important modulation effect on the ENSO–EAWM relationship on low-frequency timescales; the negative correlation between ENSO and EAWM is remarkably enhanced when they are in phase (Kim et al., 2014b). For the East Asian summer monsoon (EASM) system, a decadal variation in the EASM–ENSO connection occurred in the mid-1990s (Yim et al., 2008), and the decadal shift of the summer rainfall variability over southern China after the mid-1990s is also related to the tropical Pacific SST distribution through wave-like trains from both the western Pacific and Eurasia to East Asia (Chang et al., 2014).

In addition to the SST contribution, East Asian winter climate is greatly influenced by changes in Arctic sea-ice cover (Honda et al., 2009; Wu et al., 2011; Liu et al., 2012; Li and Wang, 2014; Li et al., 2015c; Wang et al., 2015b; Wang and Liu, 2016) and Eurasian snow (Gong et al., 2003; Cohen et al., 2007; Xin et al., 2014; Xu et al., 2017) during autumn and winter. Yeo et al. (2014) indicated that the recent climate variability in the Bering and Chukchi Seas induced by recent diminishing sea-ice cover is strongly connected with large-scale climate patterns in the Pacific. Sea-ice reduction in the Barents–Kara Seas is responsible for recent severe winters through eliciting vertical propagation of planetary waves and the subsequent weakening of the stratospheric polar vortex (Kim et al., 2014a) and downstream response of cyclonic activity (Tang et al., 2013). Liu et al. (2012) revealed that declining autumn Arctic sea ice induces much broader meridional meanders of atmospheric circulations at midlatitudes and more frequent blocking episodes that generate heavy snowfall in the European winter. Eurasian snow cover has been widely considered as an important predictor of East Asian winter climate due to its significant impacts on atmospheric circulations through regional or large-scale radiative budgets (Jeong et al., 2011; Furtado et al., 2015). High October Eurasian snow cover extent is generally accompanied by a weakened polar vortex, a negative Arctic Oscillation (AO), and cold spells in winter through stationary planetary wave activities (Cohen et al., 2007, 2012). From the perspective of vertical-propagating planetary waves with zonal wavenumber-1, however, Xu et al. (2017) argued the influence of reduced October northern Eurasian snow cover on the "warm Arctic–cold Eurasia" pattern in the following January.

Early studies mostly focused on seasonal mean climate anomalies, paying little attention to subseasonal variability (Wang et al., 2000; Cohen et al., 2012; Kug et al., 2015). However, observational evidence shows that a reverse variability in winter climate on the subseasonal timescale sometimes occurs over East Asia, resulting in huge economic losses and severe social impacts. For example, in January 2015, the surface air temperature (SAT) in China reached another historical high record (Wang et al., 2015a), while cold conditions prevailed in December 2014, with the amplitude of temperature anomalies reaching approximately 5°C. Furthermore, as part of the present work we noticed that in winter 2014/15 the Pacific SST anomalies resembled El Niño conditions in the central and eastern tropical Pacific, along with a positive PDO phase in the extratropical North Pacific. Meanwhile, a dramatic reduction in sea-ice cover over the Laptev–East Siberian Sea occurred in autumn 2014. The opposite sign in December and January–February SAT anomalies in the same context of winter Pacific SST and autumn Arctic sea-ice anomalies motivated us to consider that the effect of winter tropical Pacific SST variability (autumn Arctic sea-ice changes) might be different on the subseasonal timescale under the positive phase of PDO modulation. Therefore, in this study we attempt to explore how the winter warm Niño4 phase (autumn Arctic sea-ice reduction) exerted an influence on the East Asian SAT in the early and late winter of 2014/15 under the modulation of a positive PDO phase, an understanding of which might be helpful for climate prediction on the subseasonal timescale.

2. Data and methods

Five datasets are used in this study: (1) NCEP atmospheric reanalysis data at a resolution of 2.5° (Kalnay et al., 1996), including sea level pressure (SLP), SAT, 850-hPa zonal and meridional wind (UV850), 500-hPa geopotential height (GPH500), and 200-hPa zonal wind (U200); (2) ERA-Interim data at a resolution of 2.5° (Simmons et al., 2006), including 300-hPa zonal wind (U300) and SST; (3) ERSST.v3 data at a resolution of 2.0° (Smith et al., 2008); (4) HadISST1 data at a resolution of 1.0° (Rayner et al., 2003); and (5) six and five models from phase 5 of the Coupled Model Intercomparison Project (CMIP5) (Table 1), according to the availability of output data from the historical simulations. In this paper, the observed anomalies in 2014/15 are relative to

Table 1. List of the (a) six and (b) five CMIP5 models, whose historical simulations were employed in this study for Niño4 SST and LE-SIC, respectively, along with their group names.

Model name	Modeling center or group
(a) Nino4 SST	
BCC_CSM1.1	Beijing Climate Center, China Meteorological Administration
CSIRO MK3.6.0	Commonwealth Scientific and Industrial Research Organization in collaboration with Queensland Climate Change Centre of Excellence
FGOALS-g2	Institute of Atmospheric Physics, Chinese Academy of Sciences
GFDL CM3	NOAA Geophysical Fluid Dynamics Laboratory
GFDL-ESM2G	NOAA Geophysical Fluid Dynamics Laboratory
NorESM1-M	Norwegian Climate Centre
(b) LE–SIC	
CCSM4	National Center for Atmospheric Research
GFDL-ESM2G	NOAA Geophysical Fluid Dynamics Laboratory
GISS-E2-R	NASA Goddard Institute for Space Studies
IPSL-CM5A-LR	L'Institute Pierre-Simon Laplace
NorESM1-M	Norwegian Climate Centre

the climatology of 1979/80–2014/15.

The December, January and February PDO indices are obtained from http://research.jisao.washington.edu/pdo/. The December, January and February Niño4 indices are defined as the area-averaged SST anomalies in (5°S–5°N, 160°E–30°W). The September–October Laptev–East Siberian sea-ice cover (LE-SIC) index is defined as the area-averaged sea-ice cover anomalies for (72°–82°N, 90°–180°E) (black frame in Fig. 4d). All the defined indices are standardized. To emphasize the interannual variability, the linear trend is removed from all data and indices prior to the correlation and composite analyses. The correlation coefficients between the Niño4 and September–October LE-SIC indices are 0.07 in December, 0.14 in January, and 0.16 in February, suggesting that the impacts of winter Niño4 SST anomalies and autumn LE-SIC reduction on the East Asian winter climate are independent of each other.

To investigate the interdecadal modulation of the positive PDO phase on winter warm Niño4 SST anomalies (autumn Arctic sea-ice reduction), the PDO index is applied by a 5-yr running mean to extract a decadal variability of PDO. High and low Niño4 (LE-SIC) cases are determined when the Niño4 (LE-SIC) index is above and below standard deviations of 0.5 and −0.5, respectively. Positive and negative PDO (PDO|+ and PDO|–) phases correspond to cases in which the 5-yr running mean PDO index is above and below zero, respectively. The classification of high and low Niño4 (LE-SIC) years according to the different phases of PDO is shown in Table 2a (2b). We categorize high PDO conditions when the 5-yr running mean PDO index is above a standard deviation of 0.5 (Table 2c).

3. Subseasonal reversal of SAT variability over East Asia in winter 2014/15

Figure 1 illustrates the subseasonal (December, January and February) SAT anomalies over East Asia in winter 2014/15 relative to the winter average for the period of 1979/80–2014/15, and presents the corresponding SAT indices (defined in the following analysis). In December 2014, there are negative SAT anomalies (below −3°C) in East Asia (including China, Korea and Japan) and the western North Pacific (Fig. 1a). Apart from the weak negative values over southern Japan and the western North Pacific (below −1°C), positive SAT anomalies dominate in most parts of East Asia (including China and Korea) in January 2015, with the highest values in northern China (above 5°C) (Fig. 1b). Moreover, the spatial pattern in February 2015 largely resembles that in January 2015, with a relatively weak magnitude of 2°C (Fig. 1c). The configurations of the SAT anomalies in December 2014 and January–February 2015 tend to reveal a subseasonal reversal in SAT variability. To further validate the reversed SAT anomaly pattern, we define an SAT index based on the area-averaged SAT in East Asia [(25°–54°N, 105°–143°E) and (37°–54°N, 73°–105°E); black frames in Figs. 1a–c]. The normalized East Asian SAT indices for De-

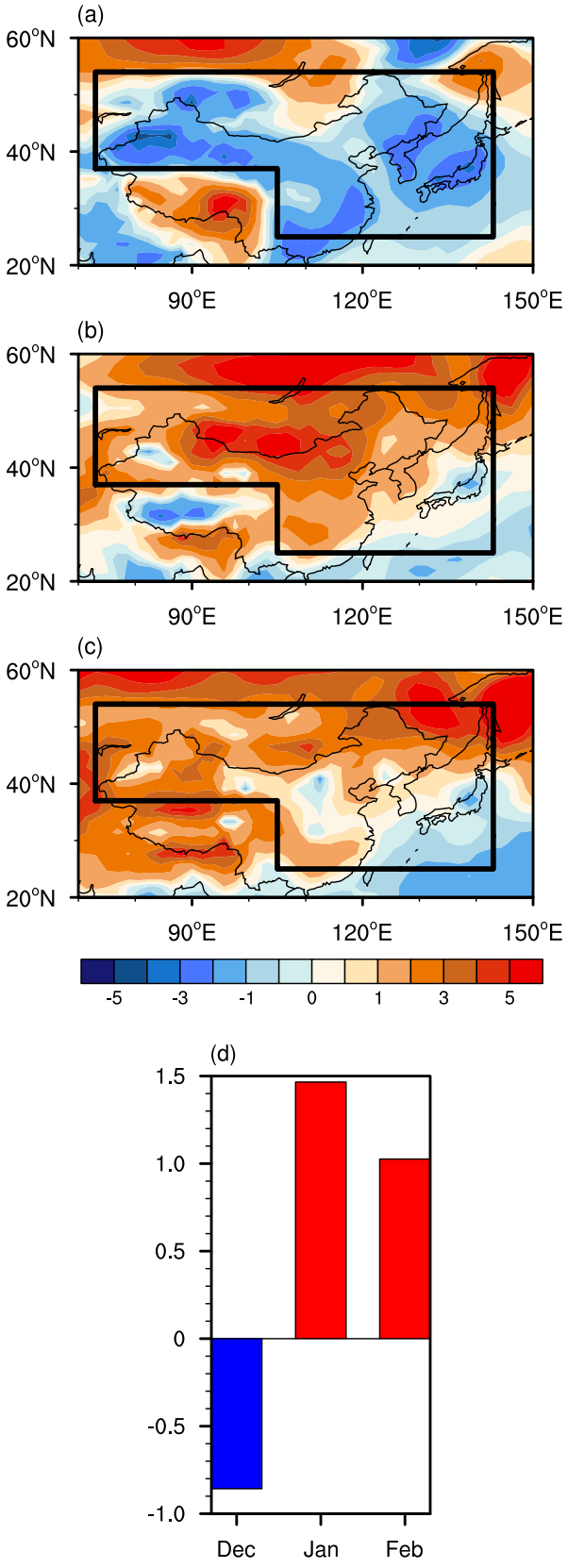

Fig. 1. (a) December, (b) January and (c) February SAT anomalies (units: °C) in winter 2014/15, and (d) December, January and February SAT indices in winter 2014/15, relative to the climatology of 1979/80–2014/15.

Table 2. Selected anomalous years based on the (a) Niño4 and (b) LE-SIC indices under different PDO phases, and (c) high December PDO conditions.

(a) Niño4 indices under different PDO phases

	Niño4 (PDO|+)		Niño4 (PDO|–)	
	High	Low	High	Low
Dec	1982, 1986, 1987, 1997, 2002, 2003, 2004, 2014	1983, 1984, 1988	1990, 1991, 1994, 2006, 2009	1998, 1999, 2000, 2007, 2008, 2010, 2011
Jan	1983, 1987, 1988, 1995, 2003, 2004, 2005, 2015	1984, 1985, 1986, 2006	1991, 1992, 1993, 1998, 2007, 2010	1989, 1999, 2000, 2001, 2008, 2009, 2011, 2012
Feb	1980, 1983, 1987, 1995, 1998, 2003, 2004, 2005, 2015	1984, 1985, 2006	1991, 1992, 1993, 2007, 2010	1989, 1999, 2000, 2001, 2008, 2009, 2011, 2012

(b) LE-SIC indices under different PDO phases

	LE-SIC (PDO|+)		LE-SIC (PDO|–)	
	Low	High	Low	High
Dec	1981, 1982, 2005, 2014	1987, 1992, 1997, 2001, 2002, 2004, 2013	1990, 1991, 1995, 2007, 2011, 2012	1996, 1998, 1999, 2000
Jan	1982, 1983, 1996, 2006, 2015	1988, 1997, 2002, 2003, 2005, 2014	1991, 1992, 2008, 2012, 2013	1993, 1998, 1999, 2000, 2001
Feb	1982, 1983, 1996, 2006, 2015	1988, 1997, 1998, 2003, 2005, 2014	1991, 1992, 2008, 2012, 2013	1993, 1999, 2000, 2001, 2002

(c) High December PDO conditions

	PDO (High)
Dec	1981, 1982, 1983, 1984, 1985, 1986, 1987, 2002, 2003, 2014

cember, January and February are −0.9, 1.5 and 1.0, respectively (Fig. 1d), implying a colder December and warmer January–February.

Figure 2 is the same as Fig. 1, but displays SLP, UV850, SH indices, and EAWM indices (defined in the following analysis). In December 2014, positive SLP anomalies are located in (80°–120°N, 40°–60°E), where the SH domain is (Wu and Wang, 2002), suggesting a strengthened SH; negative values are observed over Japan and the eastern North Pacific (Fig. 2a; shaded). In the wind field, anomalous northerly surface winds prevail along the eastern flank of the SH (Fig. 2a; vectors), indicating that the prevailing northerlies that convey cold air from high latitudes to East Asia are strengthened (He and Wang, 2012). In contrast, the SH is suppressed in January 2015 because of the negative SLP anomalies over the Asian continent and the eastern North Pacific (Fig. 2b; shaded), accompanied by anomalous southerly winds along the eastern flank (i.e., the weakened EAWM; Fig. 2b; vectors). The SLP pattern in February is similar to that in January, and mid- to high-latitude Asia is occupied by anomalous southwesterly and southeasterly winds (Fig. 2c; vectors). We employ an SH index defined by the area-averaged SLP of (40°–60°N, 80°–120°E) (Wu and Wang, 2002) and an EAWM index defined by the area-averaged 850-hPa wind speed of (25°–50°N, 115°–140°E) (Wang and Jiang, 2004). The SH indices in December, January and February are 0.7, −1.3 and −0.6, respectively, and the EAWM indices are 2.3, −0.3 and −0.7, respectively (Fig. 2d). That is, the low-level atmospheric circulation anomalies in the Asian–western North Pacific region reverse on the subseasonal timescale, consistent with the East Asian SAT variability. Furthermore, the East Asian SAT indices and SH indices are highly correlated, with coefficients of −0.77 in December, −0.85 in January, and −0.81 in February (above the 99% confidence level) for the period 1979/80–2014/15.

The subseasonal U200 climatology during 1979/80-2014/15, U200 anomalies in winter 2014/15 relative to the average of winters 1979/80-2014/15, and the corresponding EAJS indices [defined by Li and Yang (2010)] are provided in Fig. 3. Positive U200 anomalies extend from the North Pacific to northern China in December (Fig. 3a; shaded), suggesting an acceleration and westward extension of the EAJS that is usually centered near southern Japan in the wintertime (Figs. 3a–c; contours). In January–February 2015, the EAJS decelerates as negative U200 anomalies are observed in China, Japan, and the western North Pacific (Figs. 3b and c; shaded). The corresponding EAJS indices in December, January and February are 2.4, −1.1 and −1.4, respectively (Fig. 3d). Concomitant with low-level circulation variations, the upper-level circulation anomalies are also of opposite sign in December 2014 and January–February 2015. Taken together, in winter 2014/15, December East Asian cold condi-

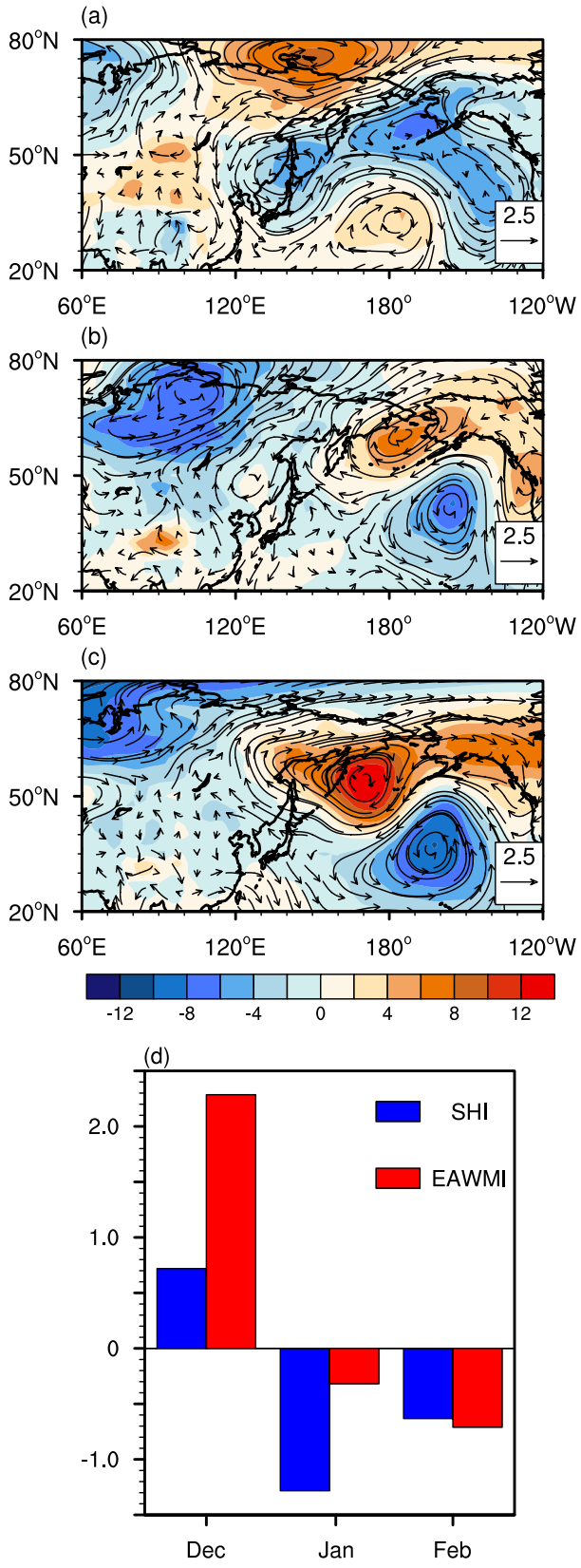

Fig. 2. (a) December, (b) January and (c) February SLP anomalies (shaded; units: hPa) and UV850 anomalies (vectors; units: m s^{-1}) in winter 2014/15, and (d) December, January and February SH indices and EAWM indices in winter 2014/15, relative to the climatology of 1979/80–2014/15.

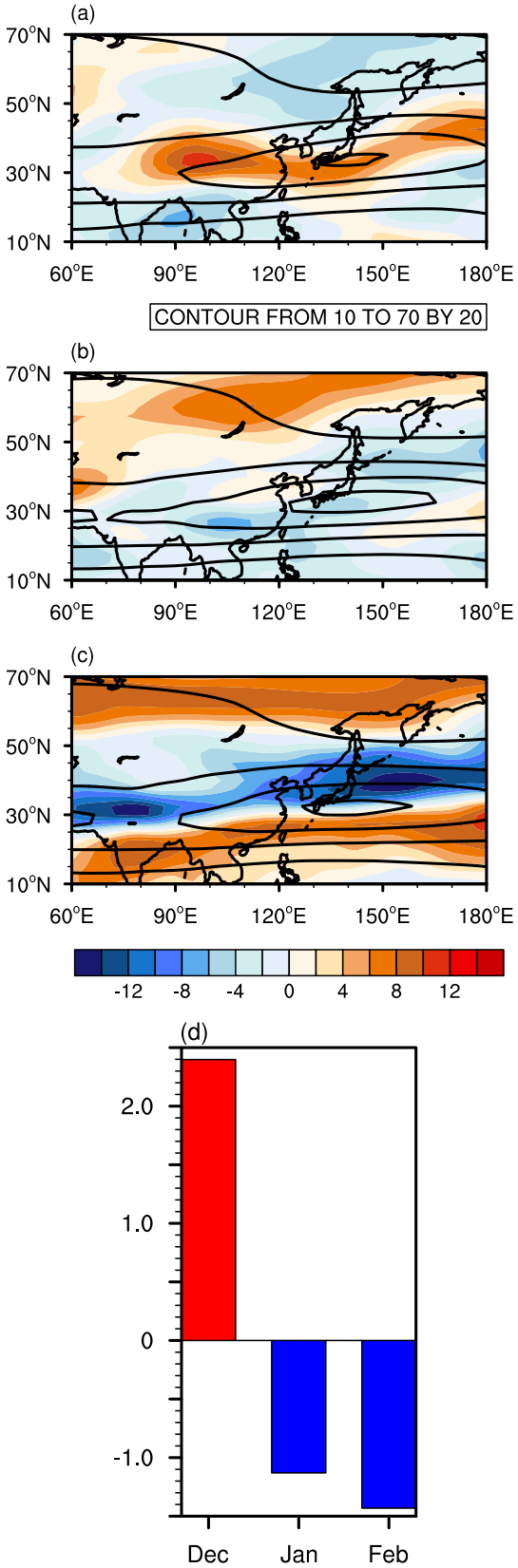

Fig. 3. (a) December, (b) January and (c) February U200 climatology (contours; units: m s^{-1}) during 1979/80–2014/15 and U200 anomalies (shaded; units: m s^{-1}) in winter 2014/15, and (d) December, January and February EAJS indices in winter 2014/15, relative to the climatology of 1979/80–2014/15.

tions are associated with the strengthened SH, enhanced surface northerlies, and an accelerated and westward-extended EAJS; warm anomalies in January–February are also closely related to the suppressed SH, weakened low-level northerlies, and a decelerated EAJS. Wang et al. (2010) suggested that the EAWM includes southern and northern modes. Interestingly, the time series of the southern mode also indicated that the EAWM experienced subseasonal diversity in winter 2014/15, with a negative temperature anomaly in December and positive temperature anomaly in January and February (figures not shown). This suggests that the subseasonal reversal of East Asian SAT variability might be related to the southern mode.

4. Possible influences of winter Pacific SST anomalies and autumn Laptev–East Siberian sea-ice reduction on East Asian SAT variability

The left-hand panel of Fig. 4 illustrates the subseasonal SST anomalies in winter 2014/15 relative to the winter average of 1979/80–2014/15. We note that the common characteristics from December 2014 to February 2015 are negative SST anomalies in the western-central North Pacific (below −1.2°C), with positive anomalies along the western coast of North America (Figs. 4a–c). In the tropical Pacific, warm SST anomalies appear with the highest values in the Niño4 region (above 0.9°C in December, 1.2°C in January–February; black frames in Figs. 4a–c). The SST anomaly pattern in the tropical and subtropical Pacific implies the concurrence of a PDO|+ phase and warm Niño4 SST anomalies. Figure 4d reveals the Arctic sea-ice cover anomalies in September–October 2014, relative to the average of September–October 1979–2014. In 2014, autumn sea-ice cover shows a reduction, with the highest values in the Laptev–East Siberian Sea (below 1500 km^2; black frame in Fig. 4d).

4.1. *How do the PDO|+ phase and Niño4 SST anomalies influence January–February SAT variability?*

The left-hand panel of Fig. 5 illustrates the composite subseasonal zonal-mean mass stream function anomalies between high and low Niño4 cases (based on a standard deviation of 0.5; Table 2a) under a PDO|+ phase. As we can see, the Hadley cell in the Northern Hemisphere is relatively weak in December, with an insignificant positive anomaly center in the low troposphere in the tropical region (0°–15°N) (Fig. 5a). In January–February, the Hadley cell develops along with a significant Ferrel cell: the positive anomaly center in the tropical region extends vertically into the upper troposphere, with a negative anomaly center in the low- to mid-troposphere in the subtropical region (15°–35°N) (Figs. 5b and c). It has been documented that El Niño is linked to an intensified Hadley cell through surface heating at the equator (Li et al., 2015b); in this sense, the enhanced Hadley cell and Ferrel cell in January–February may represent a subseasonal delay of tropical surface heating, i.e., a stronger coupling between the warm Niño4 phase and extratropical circulations in January–February relative to the weaker coupling in December. The right-hand panel of Fig. 5 displays the evolution of composite SST anomalies (150°E–160°W mean) and U300

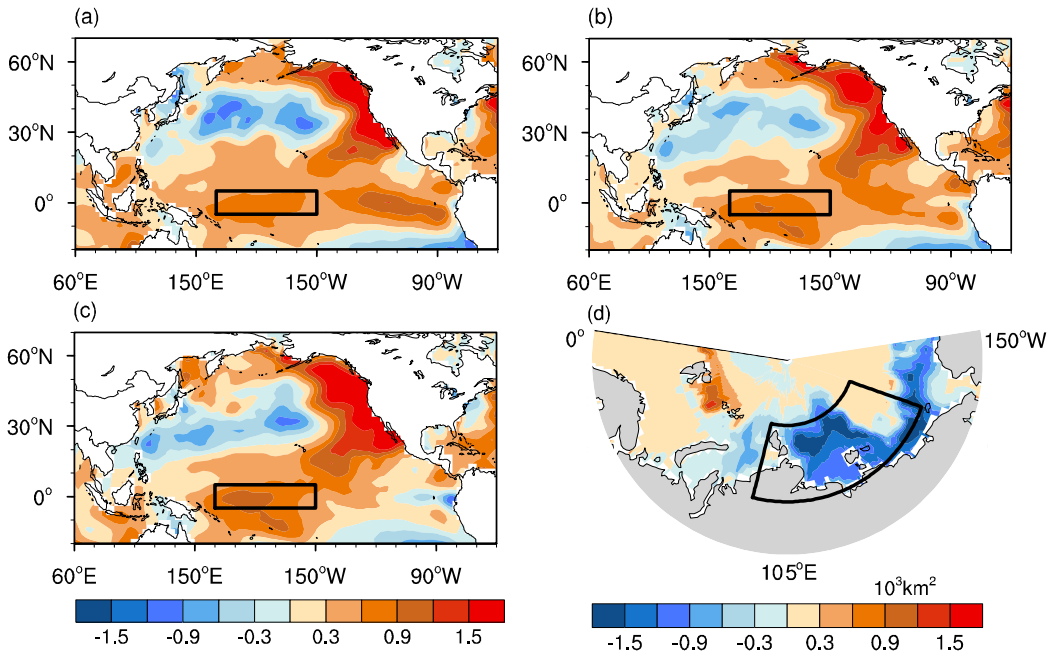

Fig. 4. (a) December, (b) January and (c) February SST anomalies (units: °C) in winter 2014/15, and (d) September–October sea-ice extent anomalies (units: 10^3 km^2) in 2014, respectively, relative to the climatology of 1979/80–2014/15.

anomalies (60°E–120°W mean) between December high and low Niño4 cases during the PDO|+ phase. Statistically significant negative SST anomalies develop in the subtropics (20°N–35°N) in December, which lessen the north–south temperature gradient, thereby suppressing the development of the subtropical westerly jet (Li et al., 2015b), which shifts slightly southward (15°N–25°N) in January–February (Fig. 5d). As a result, under the regulation of the PDO|+ phase, there is less acceleration of the Northern Hemisphere westerly jet in December relative to January–February (Fig. 5e).

We further present the subseasonal U200 anomalies between high and low Niño4 cases under a PDO|+ phase in Fig. 6. The common characteristics exhibited in January–February are the significant "positive–negative–positive" U200 anomaly bands from lower (south to 10°N) to higher (north to 70°N) latitudes over East Asia, indicative of a decelerated EAJS and stronger zonal wind speed to the south and north of the EAJS. What distinguishes December are less significant negative values in northern China–southern Japan, within the EAJS domain (Yang et al., 2002). As Zhang et al. (1997) once suggested an abnormally weak EAJS during El Niño events, the difference of the EAJS in December and January–February further supports the idea of a delayed linkage between warm Niño4 SST anomalies and extra-

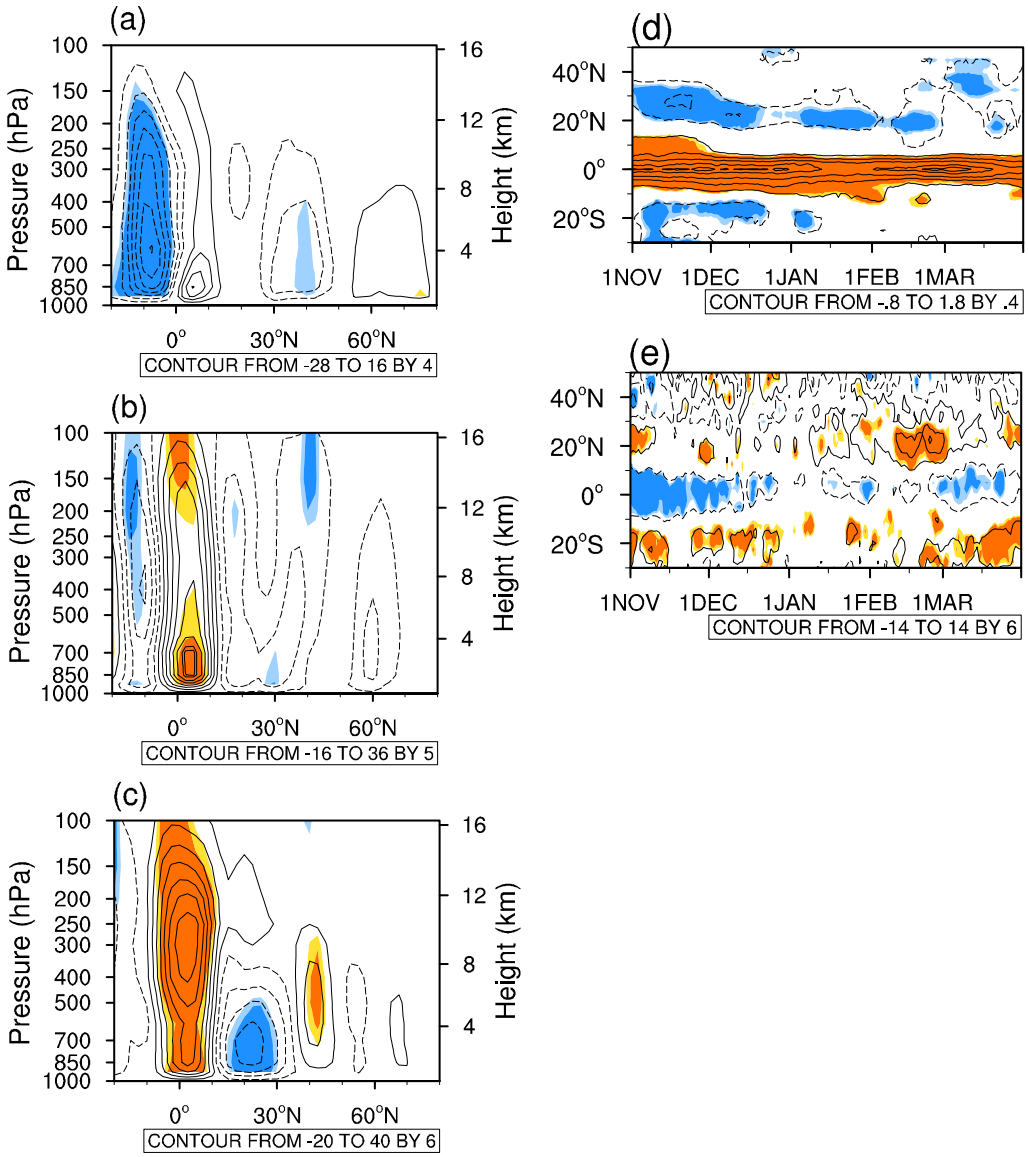

Fig. 5. Composite maps of the differences in the zonal-mean mass stream function (units: 10^9 kg s^{-1}) between high and low Niño4 cases under a PDO|+ phase in (a) December, (b) January and (c) February during 1979/80–2014/15. Evolution of the composite differences of (d) SST anomalies (150°E–160°W mean; units: °C) and (e) U300 anomalies (60°E–120°W mean; units: m s^{-1}) in December between high and low Niño4 cases under a PDO|+ phase during 1979–2014. Light and dark shaded values are significant at the 90% and 95% confidence levels, respectively, based on the Student's *t*-test.

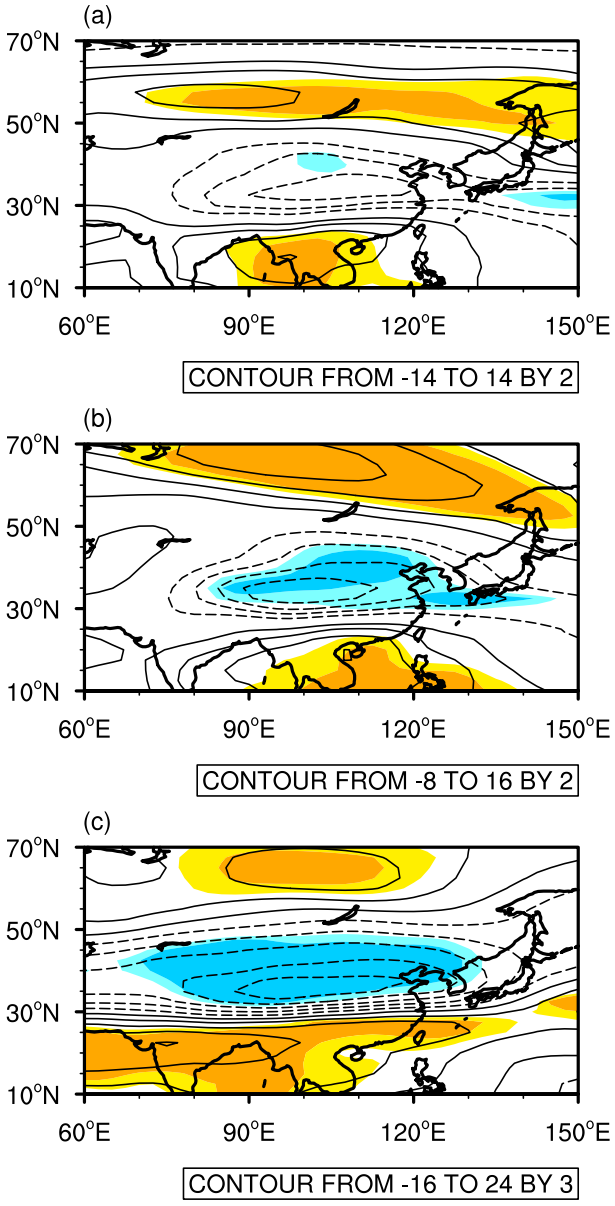

Fig. 6. Composite maps of the differences in U200 (units: m s^{-1}) between high and low Niño4 cases under a PDO|+ phase in (a) December, (b) January and (c) February, during 1979/80–2014/15. Light and dark shaded values are significant at the 90% and 95% confidence levels, respectively, based on the Student's *t*-test.

tropical atmospheric circulations under the modulation of a PDO|+ phase, which disappears under a PDO|– phase (figure not shown). According to earlier studies (Jhun and Lee, 2004; He and Wang, 2013b), such a significant upper-tropospheric "positive–negative–positive" anomaly pattern in January–February may lead to a weaker meridional shear of the EAJS and weaker surface northerlies in January–February.

The next diagnostic is generated by presenting the corresponding 1000-hPa stream function and SAT (Fig. 7). A notable discrepancy over Siberia is the anomalous cyclonic circulation observed only in January–February, which manifests the subseasonal variability of the SH and a weakened one in January–February (Figs. 7a–c). The anticyclone in the western North Pacific also shows a subseasonal variability (Figs. 7a–c). In the SAT field, it is apparent that statistically significant warm anomalies dominate over most of East Asia in January–February, while fewer significant values occur in December (Figs. 7d–f). To conclude, under the modulation of a PDO|+ phase, the subseasonal delay of tropical surface heating associated with warm Niño4 SST anomalies may result in strong Hadley and Ferrel cells in January–February, which are responsible for the coupling between the tropical and extratropical regions. Consequently, the decelerated EAJS coincides with the weakened SH and warm conditions over East Asia in January–February.

4.2. *How do the PDO|+ phase and Laptev–East Siberian sea-ice reduction influence December SAT variability?*

Figure 8 illustrates the evolution of composite SST anomalies (120°E–180° mean) and U300 anomalies (60°E–120°W mean) under high PDO conditions in December (based on a standard deviation of 0.5; Table 2c) (top panel), and between December low and high LE-SIC cases under the PDO|+ phase (based on a standard deviation of 0.5; Table 2b) (bottom panel), respectively. Under high PDO conditions, cold SST anomalies in the western North Pacific persist from November to the following March and become the most significant in December (Fig. 8a). The response of atmospheric circulation to such strong SST variability is characterized by an accelerated westerly jet in December through an enlarged meridional temperature gradient (Fig. 8b). In addition, under the coincidence of a PDO|+ phase and September–October LE-SIC declines, cold SST anomalies remain in the western North Pacific in winter, accompanied by a statistically enhanced westerly jet in December (Figs. 8c and d). That is, the relationship between sea-ice loss and the westerly jet might be modulated by a PDO|+ phase on the subseasonal timescale.

To clarify the regulation from the PDO|+ phase, we display the composite subseasonal U200 anomalies (left-hand panel) and the GPH500 and horizontal wave activity flux anomalies [computed according to the equation from Takaya and Nakamura (2001)] (right-hand panel) between low and high LE-SIC cases under the PDO|+ phase in Fig. 9. The "negative–positive–negative" U200 anomaly structure from the lower (south to 10°N) to higher latitudes (north to 60°N) over East Asia occurs only in December (Fig. 9a), which is consistent with Fig. 8d, and indicates an accelerated and westward-shifted EAJS and weaker zonal wind speed to the south and north of it. As depicted in Li et al. (2014), the reduction in autumn sea-ice cover is responsible for the westward penetration of the EAJS, exciting the rearrangement of eastward-propagating Rossby waves with a much wider horizontal structure. In this sense, the acceleration and westward shift of the December EAJS may be conducive to the propagation of Rossby waves induced by the decreased sea-ice cover through wave–mean flow interaction (Wallace, 2000;

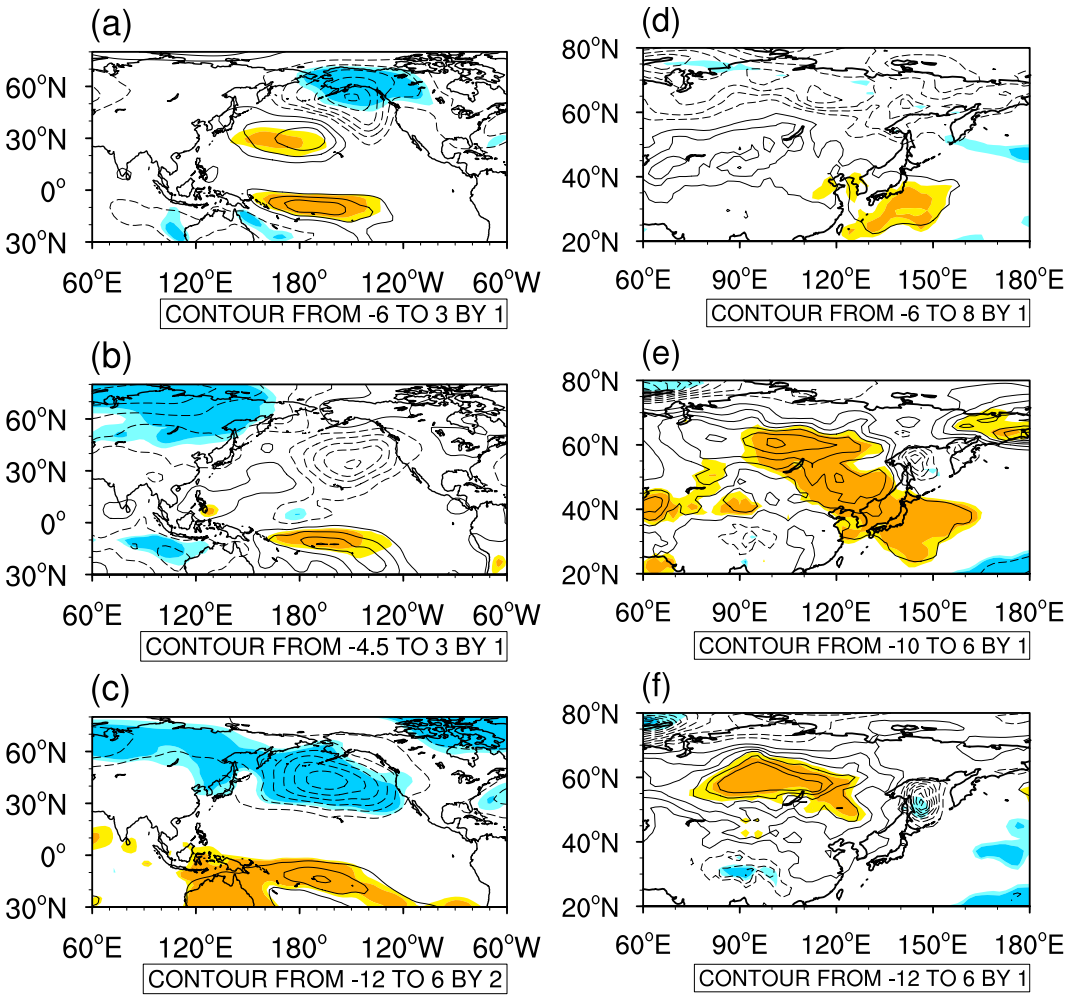

Fig. 7. Composite maps of the differences in the 1000-hPa stream function (units: 10^6 m^2 s^{-1}) between high and low Niño4 cases under a PDO|+ phase in (a) December, (b) January and (c) February, during 1979/80–2014/15. (d–f) As in (a–c) but for SAT (units: °C). Light and dark shaded values are significant at the 90% and 95% confidence levels, respectively, based on the Student's *t*-test.

Honda et al., 2009). As shown in Fig. 9d, the GPH500 response displays a remarkable wave pattern, with "negative–positive–negative" anomaly centers in Europe, central Asia, and East Asia (contours); a stationary Rossby wave train that propagates eastward from Europe to East Asia can also be estimated from the divergence of wave activity flux (vectors). The configurations of the EAJS and wave activities suggest robust polar–extratropical coupling and a strong influence of reduced autumn sea-ice cover on the East Asian climate in December during the PDO|+ phase. Under the PDO|– phase, the connection between changes in sea-ice cover and EAJS/wave activities becomes much weaker (figure not shown).

For the corresponding low-level circulation and SAT variability, in December, the positive SLP anomalies in the SH domain and negative SLP anomalies over the Sea of Japan increase the pressure gradient in the East Asia–western North Pacific region, and favor anomalous northerly winds and significant low temperatures over East Asia (Figs. 10a and d). In January–February, the anomalous SLP and SAT are quantitatively smaller and become insignificant (Figs. 10b and c, 10 and f). Taken together, under a PDO|+ phase, autumn LE-SIC reduction is associated with the westward shift of the EAJS and subsequently the eastward propagation of Rossby waves in December, which is responsible for the coupling between the polar and extratropical regions. As a result, the accelerated and westward-shifted EAJS concurs with a deepened East Asian trough (Fig. 9d), strengthened SH and significant cold conditions over East Asia in December.

5. Results based on CMIP5

The results mentioned above suggest that, under the modulation of the PDO|+ phase, changes in winter SST of the Niño4 region and autumn Arctic sea-ice cover may contribute to cold conditions in December and warm anomalies in January–February.

In this section, we use the CMIP5 historical simulations to further test our hypothesis. We select six (five) models from CMIP5 (see Table 1), in which the response of winter

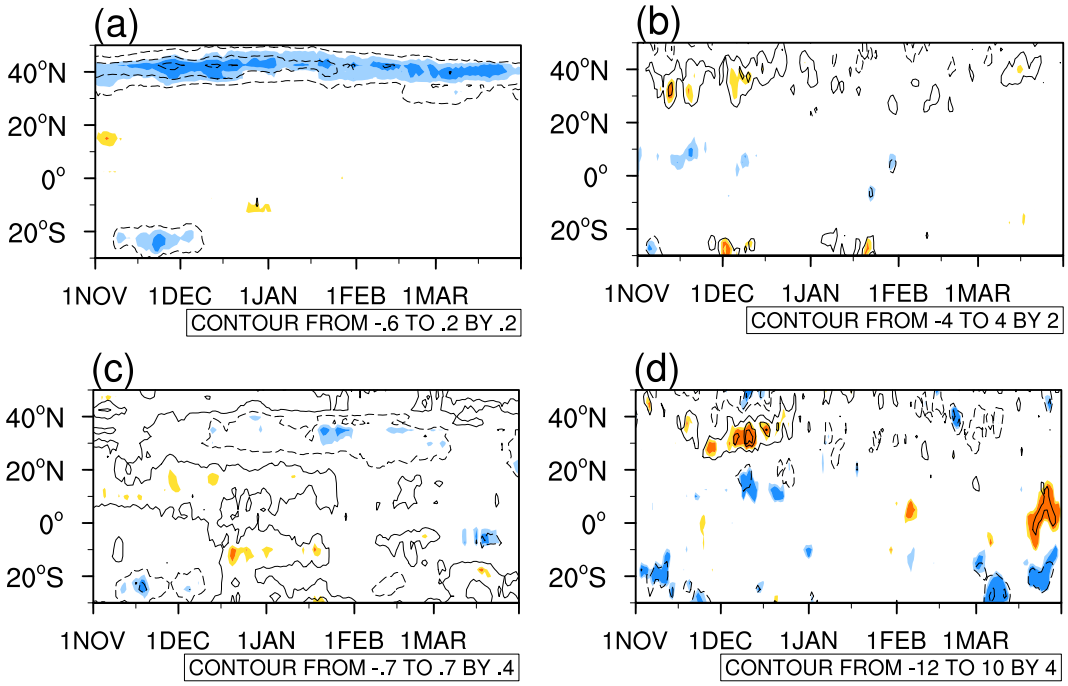

Fig. 8. Evolution of the composite differences in (a) SST anomalies (120°E–180°E mean; units: °C) and (b) U300 anomalies (60°E–120°W mean; units: m s^{-1}) in December under high PDO conditions during 1979–2014. (c, d) As in (a, b) but between low and high LE-SIC cases under PDO|+. Light and dark shaded values are significant at the 90% and 95% confidence levels, respectively, based on the Student's *t*-test.

SAT variations over East Asia to warm Niño4 phase (autumn LE-SIC reduction) under the PDO|+ phase for the period of 1979/80–2004/05 are successfully captured. When the winter warm Niño4 phase (autumn LE-SIC reduction) occurs with the PDO|+ phase, the spatial correlation coefficient of SAT in the region of (20°–80°N, 60°–180°E) between the reanalysis data and the six (five) model simulations is 0.43 (0.24).

Figure 11 illustrates the ensemble-mean SAT anomalies composited with the LE-SIC and Niño4 indices, respectively, during the PDO|+ phase. As expected, for the LE-SIC reduction, in December only, the simulated SAT anomalies show negative values from the east of Lake Baikal to coastal East Asia (Fig. 11a). For the warm Niño4 phase, positive SAT anomalies are located over mid- to high-latitude Eurasia in January, although the values in February are less significant (Figs. 11e and f). To some extent, the historical simulations are able to reproduce the subseasonal reversal in winter SAT variability over East Asia (cold December and warm January–February) based on the winter warm Niño-4 SST anomalies and autumn LE-SIC reduction under a PDO|+ phase.

6. Discussion

Our research focused on the remarkable reversal of the East Asian SAT anomaly in the early and later winter of 2014/15. The configurations of reduced autumn sea-ice cover in the Laptev–East Siberian Sea and warm SST anomalies in the Niño4 region under the PDO|+ phase that occurred in winter 2014/15 provide a plausible explanation for the colder-than-normal December and warmer-than-normal January–February of this year. It is well-known that certain factors, such as the AO, the western Pacific pattern (WP), the Atlantic Multidecadal Oscillation (AMO), solar activity, and Arctic warming can exert considerable influence on the East Asian winter climate. For example, the positive AO phase accounts for the occurrence of a weakened SH and EAWM (He and Wang, 2013b; He, 2015), and the interannual variation of the EAWM is significantly related to the Aleutian low associated with the WP (Park and Ahn, 2016). The positive phase of the multidecadal fluctuation of the AMO favors a milder EAWM (Li and Bates, 2007). Model studies reflect that La Niña–like events, which are closely connected with the EAWM, occur in response to peak solar years (Zhou et al., 2013). Recent regional Arctic warming also has a pronounced influence on the cold winters in East Asia (Kug et al., 2015). However, the compounding effects of these factors are far from understood.

Earlier studies indicated that the influence of the AO on the East Asian SAT can be regulated by the phase of the WP (Park and Ahn, 2016). Specifically, the AO–SAT relationship is strengthened (weakened) when the AO and WP are in-phase (out-of-phase), as a result of the significant (insignificant) zonal wavenumber-2 pattern of the EAWM-related atmospheric circulation. In addition to the decadal modulation of PDO (Kim et al., 2014b), the ENSO–EAWM relationship also varies depending on the AMO phase. La Niña events coincide with a strengthened (weakened) EAWM for a positive (negative) AMO, but the El Niño–EAWM relationship

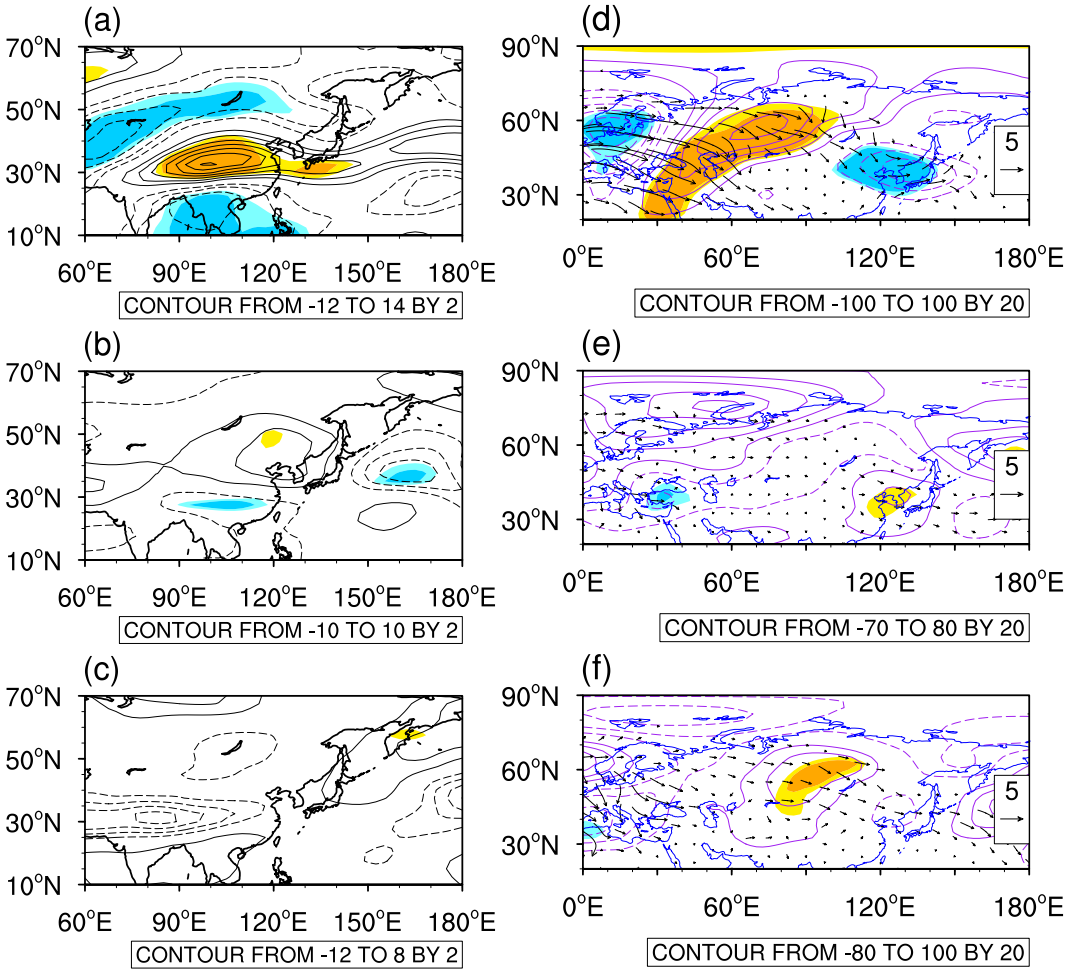

Fig. 9. Composite maps of the differences in U200 (units: m s^{-1}) between low and high LE-SIC cases under a PDO|+ phase in (a) December, (b) January and (c) February, during 1979/80–2014/15. (d–f) As in (a–c) but for GPH500 (contours; units: gpm) and the associated wave activity flux (vectors; units: m^2 s^{-2}). Light and dark shaded values are significant at the 90% and 95% confidence levels, respectively, based on the Student's *t*-test.

is irrelevant to the AMO phase (Geng et al., 2017). He and Wang (2013a) also attributed the low-frequency oscillation of the ENSO–EAWM relationship to a combination of PDO and AMO. In response to solar forcing, the ENSO-related winter climate anomaly varies with the 11-yr solar cycle and becomes significant during low solar activity winters (Zhou et al., 2013; Huo and Xiao, 2016). For January 2016, significantly colder conditions occurred over East Asia under the combined effect of the super El Niño and extreme Arctic warming, an effect that has been further verified using statistical prediction models (He et al., 2016). Therefore, the co-variability of impacts from different factors on the East Asian winter climate should be investigated in more detail in further work.

For other seasons and regions, a combined effect of different factors on the climate also exists. For example, the EASM exhibits strong interannual variation in response to ENSO (Wang et al., 2008); however, EASM variability can also be influenced by Tibetan Plateau diabatic heating through the western Pacific subtropical high (Zhang et al., 2004). Considering the forcing from the Tibetan Plateau, the EASM–ENSO relationship is highly correlated only when the Tibetan Plateau snow cover is reduced in summer (Wu et al., 2012). Lee et al. (2015) recently attributed the extreme 2013/14 winter circulation over North America to the compounding effects of the warm SST anomalies in the tropical Pacific and extratropical North Pacific and the diminished sea-ice cover in the Arctic.

In terms of PDO modulation, it is suggested that the decadal change in the intensity of the interannual variability of the South China sea summer monsoon in the 20th century (Fan and Fan, 2017) and the predictability of the interannual variation in rainfall during early summer in southern China (Duan et al., 2013) can be modulated by PDO, which are higher during a PDO|+ phase than during a PDO|– phase. Yu et al. (2015) also proposed a modulation of the "southern flood and northern drought" pattern by PDO in eastern China summers using 600-yr control simulations. The observed recent shift to a PDO|+ phase (Screen and Francis, 2016) motivated us to examine how the PDO|+ phase modu-

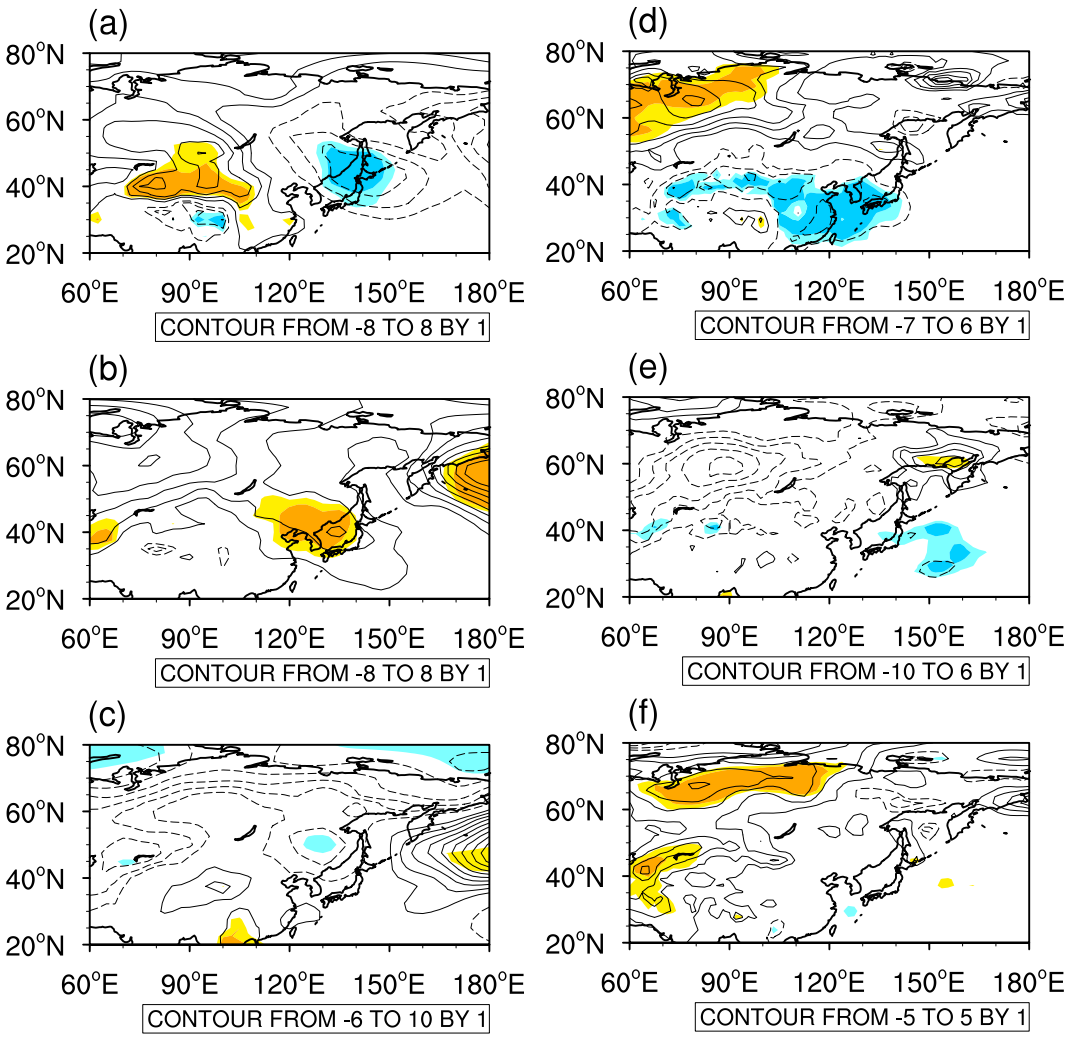

Fig. 10. Composite maps of the differences in SLP (units: hPa) between low and high LE-SIC cases under a PDO|+ phase in (a) December, (b) January and (c) February, during 1979/80–2014/15. (d–f) As in (a–c) but for SAT (units: °C). Light and dark shaded values are significant at the 90% and 95% confidence levels, respectively, based on the Student's *t*-test.

lates the influences of warm Niño4 SST anomalies and Arctic sea-ice reduction on the winter SAT variability over East Asia on the subseasonal time scale. As depicted in Li et al. (2015a), however, extratropical ocean warming plays an important role in changes in the winter circulation in the Arctic. Much more research is needed on the interdecadal modulation by the PDO|– phase.

7. Summary

In this study, we found that in the early winter of 2014/15 the surface temperature over East Asia was lower than normal, whereas in the late winter of 2014/15 the surface temperature was higher than normal. Simultaneously, PDO was in its positive phase, autumn sea-ice cover in the Laptev–East Siberian Sea was lower than normal, and a warm Niño4 phase occurred. We explored the influence of winter warm Niño4 SST anomalies (autumn Arctic sea-ice reduction) on the subseasonal reversal of SAT variability over East Asia under the decadal PDO|+ condition. The results showed the following:

(1) Under the modulation of a PDO|+ phase, warm Niño4 SST anomalies can induce a subseasonal delay of tropical surface heating, and hence a strong January–February Hadley cell and Ferrel cell, which are responsible for the coupling between tropical SST anomalies and extratropical atmospheric circulation. The resulting "positive–negative–positive" anomaly pattern in U200 suggests weakened meridional shear of the EAJS, and favors a situation in which the northerlies and SH are weakened. Therefore, significant warm conditions occur over East Asia in January–February.

(2) Under a PDO|+ phase, September–October LE-SIC reduction is related to significant cold SST anomalies in the western North Pacific and the subsequently larger meridional temperature gradient between the tropical and midlatitude regions. The EAJS is thereby accelerated and westward-shifted

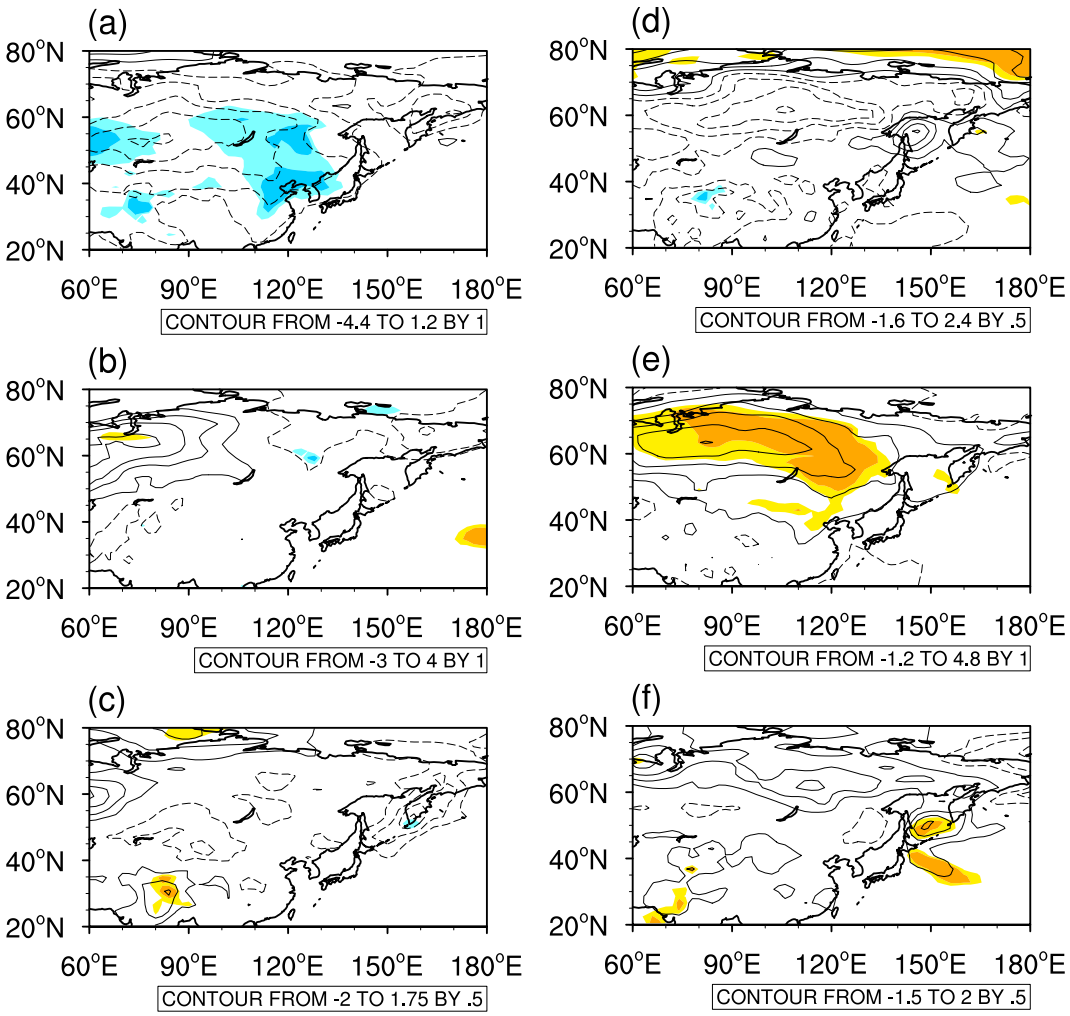

Fig. 11. Composite maps of the differences in SAT (units: °C) between low and high LE-SIC cases under a PDO|+ phase in (a) December, (b) January and (c) February, during 1979/80–2004/05, derived from the CMIP5 historical simulations. (d–f) As in (a–c) but between high and low Niño4 cases. Light and dark shaded values are significant at the 90% and 95% confidence levels, respectively, based on the Student's *t*-test.

in December, and favors the eastward propagation of Rossby waves induced by sea-ice declines that strengthen the coupling between the polar and extratropical regions. Therefore, the SH and East Asian trough are intensified and East Asia becomes colder in December.

In summary, the subseasonal reversal of East Asian SAT variability in winter of 2014/15 may be attributable to winter warm Niño4 SST anomalies and autumn Arctic sea-ice reduction under the PDO|+ phase modulation. Moreover, such a "reversal" phenomenon has sometimes occurred under similar SST anomaly patterns over the past century, such as the winters of 1913/14 and 1965/66 (figure not shown).

Acknowledgements. This research was supported by the National Key R&D Program of China (Grant No. 2016YFA0600703), the National Natural Science Foundation of China (Grant Nos. 41505073 and 41605059), the Young Talent Support Program by China Association for Science and Technology (Grant No. 2016QNRC001), and the Research Council of Norway (Grant No. SNOWGLACE #244166).

REFERENCES

Chang, E. C., S. W. Yeh, S. Y. Hong, J. E. Kim, R. G. Wu, and K. Yoshimura, 2014: Study on the changes in the East Asian precipitation in the mid-1990s using a high-resolution global downscaled atmospheric data set. *J. Geophys. Res. Atmos.*, **119**, 2279–2293, https://doi.org/10.1002/2013JD020903.

Chen, J., and S. Q. Sun, 1999: Eastern Asian winter monsoon anomaly and variation of global circulation Part I: A comparison study on strong and weak winter monsoon. *Scientia Atmospherica Sinica*, **23**, 101–110, https://doi.org/10.3878/j.issn.1006-9895.1999.01.12. (in Chinese)

Cohen, J., M. Barlow, P. J. Kushner, and K. Saito, 2007: Stratosphere and troposphere coupling and links with Eurasian land surface variability. *J. Climate*, **20**, 5335–5343, https://doi.org/10.1175/2007JCLI1725.1.

Cohen, J. L., J. C. Furtado, M. A. Barlow, V. A. Alexeev,

and J. E. Cherry, 2012: Arctic warming, increasing snow cover and widespread boreal winter cooling. *Environmental Research Letters*, **7**, 014007, https://doi.org/10.1088/1748-9326/7/1/014007.

Duan, W. S., L. Y. Song, Y. Li, and J. Y. Mao, 2013: Modulation of PDO on the predictability of the interannual variability of early summer rainfall over South China. *J. Geophys. Res. Atmos.*, **118**, 13 008–13 021, https://doi.org/10.1002/2013JD019862.

Fan, Y., and K. Fan, 2017: Pacific decadal oscillation and the decadal change in the intensity of the interannual variability of the South China Sea summer monsoon. *Atmos. Oceanic Scie. Lett.*, **10**, 162–167, https://doi.org/10.1080/16742834.2016.1256189.

Furtado, J. C., J. L. Cohen, A. H. Butler, E. E. Riddle, and A. Kumar, 2015: Eurasian snow cover variability and links to winter climate in the CMIP5 models. *Climate Dyn.*, **45**, 2591–2605, https://doi.org/10.1007/s00382-015-2494-4.

Geng, X., W. J. Zhang, M. F. Stuecker, P. Liu, F. F. Jin, and G. R. Tan, 2017: Decadal modulation of the ENSO-East Asian winter monsoon relationship by the Atlantic Multidecadal Oscillation. *Climate Dyn.*, **49**, 2531–2544, https://doi.org/10.1007/s00382-016-3465-0.

Gong, G., D. Entekhabi, and J. Cohen, 2003: Modeled Northern Hemisphere winter climate response to realistic Siberian snow anomalies. *J. Climate*, **16**, 3917–3931, https://doi.org/10.1175/1520-0442(2003)016<3917:MNHWCR>2.0.CO;2.

He, S. P., 2015: Asymmetry in the Arctic Oscillation teleconnection with January cold extremes in Northeast China. *Atmos. Oceanic Scie. Lett.*, **8**, 386–391, https://doi.org/10.3878/AOSL20150053.

He, S. P., and H. J. Wang, 2012: An integrated East Asian winter monsoon index and its interannual variability. *Chinese Journal of Atmospheric Sciences*, **36**, 523–538, https://doi.org/10.3878/j.issn.1006-9895.2011.11083. (in Chinese)

He, S. P., and H. J. Wang, 2013a: Oscillating relationship between the East Asian winter monsoon and ENSO. *J. Climate*, **26**, 9819–9838, https://doi.org/10.1175/JCLI-D-13-00174.1.

He, S. P., and H. J. Wang, 2013b: Impact of the November/December Arctic Oscillation on the following January temperature in East Asia. *J. Geophys. Res. Atmos.*, **118**, 12 981–12 998, https://doi.org/10.1002/2013JD020525.

He, S. P., H. J. Wang, and J. P. Liu, 2013: Changes in the relationship between ENSO and Asia-Pacific midlatitude winter atmospheric circulation. *J. Climate*, **26**, 3377–3393, https://doi.org/10.1175/JCLI-D-12-00355.1.

He, S. P., H. J. Wang, X. P. Xu, and J. W. Li, 2016: Impact of Arctic warming and the super El Niño in winter 2015/2016 on the East Asian climate anomaly. *Transactions of Atmospheric Sciences*, **39**, 735–743, https://doi.org/10.13878/j.cnki.dqkxxb.20161008002. (in Chinese)

Honda, M., J. Inoue, and S. Yamane, 2009: Influence of low Arctic sea-ice minima on anomalously cold Eurasian winters. *Geophys. Res. Lett.*, **36**, L08707, https://doi.org/10.1029/2008GL037079.

Huo, W. J., and Z. N. Xiao, 2016: The impact of solar activity on the 2015/16 El Niño event. *Atmos. Oceanic Scie. Lett.*, **9**, 428–435, https://doi.org/10.1080/16742834.2016.1231567.

Jeong, J. H., T. H. Ou, H. W. Linderholm, B. M. Kim, S. J. Kim, J. S. Kug, and D. L. Chen, 2011: Recent recovery of the Siberian high intensity. *J. Geophysi. Res.*, **116**, D23102, https://doi.org/10.1029/2011JD015904.

Jhun, J. G., and E. J. Lee, 2004: A new East Asian winter monsoon index and associated characteristics of the winter monsoon. *J. Climate*, **17**, 711–726, https://doi.org/10.1175/1520-0442(2004)017<0711:ANEAWM>2.0.CO;2.

Jin, C. X., T. J. Zhou, Z. Guo, B. Wu, and X. L. Chen, 2016: Improved simulation of the East Asian winter monsoon interannual variation by IAP/LASG AGCMs. *Atmospheric and Oceanic Science Letters*, **9**, 204–210, https://doi.org/10.1080/16742834.2016.1150774.

Kalnay, E., and Coauthors, 1996: The NCEP/NCAR 40-year reanalysis project. *Bull. Amer. Meteor. Soc.*, **77**, 437–471, https://doi.org/10.1175/1520-0477(1996)077<0437:TNYRP>2.0.CO;2.

Kim, B. M., S. W. Son, S. K. Min, J. H. Jeong, S. J. Kim, X. Zhang, T. Shim, and J. H. Yoon, 2014a: Weakening of the stratospheric polar vortex by Arctic sea-ice loss. *Nature Communications*, **5**, 4646, https://doi.org/10.1038/ncomms5646.

Kim, J. W., S. W. Yeh, and E. C. Chang, 2014b: Combined effect of El Niño-Southern oscillation and Pacific decadal oscillation on the East Asian winter monsoon. *Climate Dyn.*, **42**, 957–971, https://doi.org/10.1007/s00382-013-1730-z.

Kug, J. S., J. H. Jeong, Y. S. Jang, B. M. Kim, C. K. Folland, S. K. Min, and S. W. Son, 2015: Two distinct influences of Arctic warming on cold winters over North America and East Asia. *Nature Geoscience*, **8**, 759–762, https://doi.org/10.1038/ngeo2517.

Lee, M. Y., C. C. Hong, and H. H. Hsu, 2015: Compounding effects of warm sea surface temperature and reduced sea ice on the extreme circulation over the extratropical North Pacific and North America during the 2013-2014 boreal winter. *Geophys. Res. Lett.*, **42**, 1612–1618, https://doi.org/10.1002/2014GL062956.

Li, F., and H. J. Wang, 2014: Autumn Eurasian snow depth, autumn Arctic sea ice cover and East Asian winter monsoon. *International Journal of Climatology*, **34**, 3616–3625, https://doi.org/10.1002/joc.3936.

Li, F., H. J. Wang, and Y. Q. Gao, 2014: On the strengthened relationship between the East Asian winter monsoon and Arctic Oscillation: A comparison of 1950-70 and 1983-2012. *J. Climate*, **27**, 5075–5091, https://doi.org/10.1175/JCLI-D-13-00335.1.

Li, F., H. J. Wang, and Y. Q. Gao, 2015a: Extratropical ocean warming and winter Arctic sea ice cover since the 1990s. *J. Climate*, **28**, 5510–5522, https://doi.org/10.1175/JCLI-D-14-00629.1.

Li, F., H. J. Wang, and Y. Q. Gao, 2015b: Modulation of Aleutian Low and Antarctic Oscillation co-variability by ENSO. *Climate Dyn.*, **44**, 1245–1256, https://doi.org/10.1007/s00382-014-2134-4.

Li, F., H. J. Wang, and Y. Q. Gao, 2015c: Change in sea ice cover is responsible for non-uniform variation in winter temperature over East Asia. *Atmos. Oceanic Scie. Lett.*, **8**, 376–382, https://doi.org/10.3878/AOSL20150039.

Li, S. L., and G. T. Bates, 2007: Influence of the Atlantic multidecadal oscillation on the winter climate of East China. *Adv. Atmos. Scie.*, **24**, 126–135, https://doi.org/10.1007/s00376-007-0126-6.

Li, Y. Q., and S. Yang, 2010: A dynamical index for the East Asian winter monsoon. *J. Climate*, **23**, 4255–4262, https://doi.org/10.1175/2010JCLI3375.1.

Liu, J. P., J. A. Curry, H. J. Wang, M. R. Song, and R. M. Horton, 2012: Impact of declining Arctic sea ice on winter snow-

fall. *Proc. Natl. Acad. Sci.*, **109**, 4074–4079, https://doi.org/10.1073/pnas.1114910109.

Park, H. J., and J. B. Ahn, 2016: Combined effect of the Arctic Oscillation and the Western Pacific pattern on East Asia winter temperature. *Climate Dyn.*, **46**, 3205–3221, https://doi.org/10.1007/s00382-015-2763-2.

Rayner, N. A., D. E. Parker, E. B. Horton, C. K. Folland, L. V. Alexander, D. P. Rowell, E. C. Kent, and A. Kaplan, 2003: Global analyses of sea surface temperature, sea ice, and night marine air temperature since the late Nineteenth Century. *J. Geophys. Res. Atmos.*, **108**, 4407, https://doi.org/10.1029/2002JD002670.

Screen, J. A., and J. A. Francis, 2016: Contribution of sea-ice loss to Arctic amplification is regulated by Pacific Ocean decadal variability. *Nature Climate Change*, **6**, 856–860, https://doi.org/10.1038/nclimate3011.

Simmons, A. J., S. M. Uppala, D. P. Dee, and S. Kobayashi, 2006: ERA-Interim: New ECMWF reanalysis products from 1989 onwards. *ECMWF Newsletter*, **110**, 25–35.

Smith, T. M., R. W. Reynolds, T. C. Peterson, and J. Lawrimore, 2008: Improvements to NOAA's historical merged land-ocean surface temperature analysis (1880–2006). *J. Climate*, **21**, 2283–2296, https://doi.org/10.1175/2007JCLI2100.1.

Takaya, K., and H. Nakamura, 2001: A formulation of a phase-independent wave- activity flux for stationary and migratory quasigeostrophic eddies on a zonally varying basic flow. *J. Atmos. Sci.*, **58**, 608–627, https://doi.org/10.1175/1520-0469(2001)058<0608:AFOAPI>2.0.CO;2.

Tang, Q. H., X. J. Zhang, X. H. Yang, and J. A. Francis, 2013: Cold winter extremes in northern continents linked to Arctic sea ice loss. *Environmental Research Letters*, **8**, 014036, https://doi.org/10.1088/1748-9326/8/1/014036.

Wallace, J. M., 2000: North Atlantic Oscillation/annular mode: Two paradigms-one phenomenon. *Quart. J. Roy. Meteor. Soc.*, **126**, 791–805, https://doi.org/10.1256/smsqj.56401.

Wang, B., R. G. Wu, and X. H. Fu, 2000: Pacific-East Asian teleconnection: How does ENSO affect East Asian climate? *J. Climate*, **13**, 1517–1536, https://doi.org/10.1175/1520-0442(2000)013<1517:PEATHD>2.0.CO;2.

Wang, B., Z. W. Wu, J. P. Li, J. Liu, C. P. Chang, Y. H. Ding, and G. X. Wu, 2008: How to measure the strength of the East Asian summer monsoon. *J. Climate*, **21**, 4449–4463, https://doi.org/10.1175/2008JCLI2183.1.

Wang, B., Z. W. Wu, C. P. Chang, J. Liu, J. P. Li, and T. J. Zhou, 2010: Another look at interannual-to-interdecadal variations of the East Asian winter monsoon: The northern and southern temperature modes. *J. Climate*, **23**, 1495–1512, https://doi.org/10.1175/2009JCLI3243.1.

Wang, D. Q., T. Cui, D. Si, X. Shao, Q. Q. Li, and C. H. Sun, 2015a: Features and possible causes for East Asian winter monsoon in 2014/2015. *Meteorological Monthly*, **41**, 907–914, https://doi.org/10.7519/j.issn.1000-0526.2015.07.013. (in Chinese)

Wang, H. J., and D. B. Jiang, 2004: A new East Asian winter monsoon intensity index and atmospheric circulation comparison between strong and weak composite. *Quaternary Sciences*, **24**, 19–27, https://doi.org/10.3321/j.issn:1001-7410.2004.01.003. (in Chinese)

Wang, H. J., and S. P. He, 2012: Weakening relationship between East Asian winter monsoon and ENSO after mid-1970s. *Chinese Science Bulletin*, **57**, 3535–3540, https://doi.org/10.1007/s11434-012-5285-x.

Wang, H. J., H. P. Chen, and J. P. Liu, 2015b: Arctic sea ice decline intensified haze pollution in eastern China. *Atmospheric and Oceanic Science Letters*, **8**, 1–9, https://doi.org/10.3878/AOSL20140081.

Wang, S. Y., and J. P. Liu, 2016: Delving into the relationship between autumn Arctic sea ice and central-eastern Eurasian winter climate. *Atmospheric and Oceanic Science Letters*, **9**, 366–374, https://doi.org/10.1080/16742834.2016.1207482.

Wu, B. Y., and J. Wang, 2002: Winter Arctic oscillation, Siberian high and East Asian winter monsoon. *Geophys. Res. Lett.*, **29**, 3-1–3-4, https://doi.org/10.1029/2002GL015373.

Wu, Z. W., J. P. Li, Z. H. Jiang, and J. H. He, 2011: Predictable climate dynamics of abnormal East Asian winter monsoon: Once-in-a-century snowstorms in 2007/2008 winter. *Climate Dyn.*, **37**, 1661–1669, https://doi.org/10.1007/s00382-010-0938-4.

Wu, Z. W., J. P. Li, Z. H. Jiang, and T. T. Ma, 2012: Modulation of the Tibetan Plateau snow cover on the ENSO teleconnections: From the East Asian summer monsoon perspective. *J. Climate*, **25**, 2481–2488, https://doi.org/10.1175/JCLI-D-11-00135.1.

Xin, Y. F., G. Liu, and Q. H. Jin, 2014: Individual variations of winter surface air temperature over Northwest and Northeast China and their respective preceding factors. *Atmos. Oceanic Scie. Lett.*, **7**, 346–351, https://doi.org/10.1080/16742834.2014.11447188.

Xu, X. P., S. P. He, F. Li, and H. J. Wang, 2017: Impact of northern Eurasian snow cover in autumn on the warm Arctic–cold Eurasia pattern during the following January and its linkage to stationary planetary waves. *Climate Dyn.*, https://doi.org/10.1007/s00382-017-3732-8.

Yang, J. L., Q. Y. Liu, and Z. Y. Liu, 2010: Linking observations of the Asian monsoon to the Indian Ocean SST: Possible roles of Indian Ocean Basin mode and dipole mode. *J. Climate*, **23**, 5889–5902, https://doi.org/10.1175/2010JCLI2962.1. (in Press)

Yang, S., K. M. Lau, and K. M. Kim, 2002: Variations of the East Asian jet stream and Asian-Pacific-American winter climate anomalies. *J. Climate*, **15**, 306–325, https://doi.org/10.1175/1520-0442(2002)015<0306:VOTEAJ>2.0.CO;2.

Ye, F., and H. P. Chen, 2016: Warming over the North Pacific can intensify snow events in Northeast China. *Atmos. Oceanic Scie. Lett.*, **9**, 122–128, https://doi.org/10.1080/16742834.2016.1133072.

Yeo, S. R., K. Y. Kim, S. W. Yeh, B. M. Kim, T. Shim, and J. G. Jhun, 2014: Recent climate variation in the Bering and Chukchi Seas and its linkages to large-scale circulation in the Pacific. *Climate Dyn.*, **42**, 2423–2437, https://doi.org/10.1007/s00382-013-2042-z.

Yim, S. Y., J. G. Jhun, and S. W. Yeh, 2008: Decadal change in the relationship between east Asian-western North Pacific summer monsoons and ENSO in the mid-1990s. *Geophys. Res. Lett.*, **35**, L20711.

Yu, L., T. Furevik, O. H. Otterå, and Y. Q. Gao, 2015: Modulation of the Pacific Decadal Oscillation on the summer precipitation over East China: A comparison of observations to 600-years control run of Bergen Climate Model. *Climate Dyn.*, **44**, 475–494, https://doi.org/10.1007/s00382-014-2141-5.

Zhang, Y., K. R. Sperber, and J. S. Boyle, 1997: Climatology and interannual variation of the East Asian winter monsoon: Results from the 1979-95 NCEP/NCAR Reanalysis. *Mon. Wea. Rev.*, **125**, 2605–2619, https://doi.org/10.1175/1520-

0493(1997)125<2605:CAIVOT>2.0.CO;2.

Zhang, Y. S., T. Li, and B. Wang, 2004: Decadal change of the spring snow depth over the Tibetan Plateau: The associated circulation and influence on the East Asian summer monsoon. *J. Climate*, **17**, 2780–2793, https://doi.org/10.1175/1520-0442(2004)017<2780:DCOTSS>2.0.CO;2.

Zhou, Q., W. Chen, and W. Zhou, 2013: Solar cycle modulation of the ENSO impact on the winter climate of East Asia. *J. Geophys. Res. Atmos.*, **118**, 5111–5119, https://doi.org/10.1002/jgrd.50453.